From Grids to Places

M. Franzius*, R. Vollgraf†, L. Wiskott*

August 28, 2006

Hafting et al. (2005) described *grid cells* in the dorsocaudal region of the medial enthorinal cortex (dMEC). These cells show a strikingly regular grid-like firing-pattern as a function of the position of a rat in an enclosure. Since the dMEC projects to the hippocampal areas containing the well-known place cells, the question arises whether and how the localized responses of the latter can emerge based on the output of grid cells. Here, we show that, starting with simulated grid-cells, a simple linear transformation maximizing sparseness leads to a localized representation similar to place fields.

As reported by Hafting et al. (2005) grid cells in the dMEC show spatial firing patterns in the form of hexagonal grids with frequencies within one octave (39 to 73 cm mean distance), random phase shifts, and random orientations. The firing patterns of place cells in the hippocampus, on the other hand, are localized spots Muller (1996). Our hypothesis is that the latter can be generated from the former simply by sparsification, which is consistent with evidence that firing patterns in hippocampal regions CA1 and CA3 are sparser than in enthorhinal cortex (O'Reilly and McClelland, 1994).

---

*Intitute for Theoretical Biology, Humboldt-University, Berlin, Germany; {m.franzius, l.wiskott}@biologie.hu-berlin.de

†Department of Computer Science, Technical University of Berlin, Germany; vro@cs.tu-berlin.de

To show that place fields can be derived from grid-cells by sparsification we simulated a linear two-layer network. The input units were 100 simulated grid-cells of a virtual rat with activity patterns synthesized by Gaussians arranged on a hexagonal grid (Fig. 1 A). Some positional jitter, random anisotropy, and amplitude variation of the Gaussians was introduced, and white noise was added to qualitatively match the slightly irregular experimental data.

Let $g_i(\vec{r})$ denote the activity of grid-cell g_i as a function of location $\vec{r}$. Given a virtual path $\vec{r}(t)$ of a rat within the enclosure, the input into the hippocampus coming from the grid-cells is $x_i(t) := g_i(\vec{r}(t))$. To achieve sparseness we applied independent component analysis (ICA) Hyvärinen (1999b) on a set of 200.000 time points from this input by subtracting the mean and using the CuBICA algorithm, which attempts to diagonalize the tensors of third and fourth order cumulants (Blaschke and Wiskott, 2004), but we have obtained similar results with other sparsification algorithms, such as FastICA (Hyvärinen, 1999a) or simply maximizing peak activity under a unit variance, zero mean and decorrelation constraint. The sign of each output unit, which is arbitrary for ICA, was chosen such that the value with the largest magnitude is positive, and then constants c_j were added to ensure nonnegative values. This yielded an affine transformation with matrix T producing 100 output signals $y_j(t) := \sum_i T_{ji}x_i(t) + c_j$ that are maximally independent and significantly sparser than the input signals (kurtosis increased on average from 2.9 for the input units to 28.6 for the output units). The output-unit activities as a function of location are $p_j(\vec{r}) := \sum_i T_{ji}g_i(\vec{r}) + c_j$ and show localized place fields (Fig. 1, B). We measured the number of peaks in a unit's output by counting the number of distinct contiguous areas containing pixels with at least 50% of the unit's maximum activity. A large proportion of output units (76%) show a single spot of activity (Fig. 1 B, units 1, 25, 50, 75), some units (5%) show few spots (Fig. 1 B, unit 87), both being consistent with the patterns of physiological place-cells. Only few output units (19%) show patterns of activity without clear structure (Fig. 1 B, unit 100). The size of the resulting place fields is similar for most units and comparable to the size of the smallest grid-cell fields, but it also depends on the number of grid cell inputs: more inputs lead to more localized output fields, while too few inputs can increase the number of fields per output unit.

There are different ways of achieving sparseness and localized place fields. We have used ICA here and have obtained similar results by maximimizing peak activity; competetive learning schemes would presumably also work. There are other linear transformations, however, that do not lead to localized place fields. As controls we have applied random mixtures, principal component analysis (PCA), and slow feature analysis (SFA, Wiskott and Sejnowski (2002)) to the grid cell input. The latter has been chosen because Wyss et al. (2006) have presented a model based on the slowness principle that was able learn localized place cells. As one would expect with random rotations of the input, the results retain some grid structure but are less regular than the input (Fig. 1 C), but no unit has one single or two peaks of activity. With PCA the first units (i. e. those with highest variance) are highly structured and have large amplitudes, much like the grid cells themselves, while the later low-variance units have low amplitudes and are noise-like (three representative examples are shown in Fig. 1 D). None of these units had a single or two peaks of activity. From the temporal slowness objective we'd expect patterns with low spatial frequencies first, and high-frequency non-localized patterns later, when outputs are sorted by slowness (Fig. 1 E). Only 2% of these outputs have one or two peaks of activity. None of these three alternative linear transforms (Fig. 1 C-E) lead to localized place fields, which in case of SFA is somewhat inconsistent with the results from Wyss et al. (2006).

We conclude that sparse coding (achieved here by ICA, which is is linear and instantaneous) is a simple and efficient computational approach for the generation of place cells from grid cells. Other linear methods, such as PCA or linear SFA, do not work. However, the complexity of place-field generation is now only shifted to the computation of grid-cell behavior and still open for discussion.

Acknowledegements

This research was funded by the Volkswagen Foundation (MF, LW) and the Wellcome Trust (RV: 10008261).

References

Blaschke, T. and Wiskott, L. (2004). CuBICA: Independent component analysis by simultaneous third- and fourth-order cumulant diagonalization. *IEEE Transactions on Signal Processing*, 52(5):1250–1256.

Hafting, T., Fyhn, M., Molden, S., Moser, M., and Moser, E. I. (2005). Microstructure of a spatial map in the entorhinal cortex. *Nature*, 436(7052):801–806. 10.1038/nature03721.

Hyvärinen, A. (1999a). Fast and robust fixed-point algorithms for independent component analysis. *IEEE Transactions on Neural Networks*, 10:626–634.

Hyvärinen, A. (1999b). Survey on independent component analysis. *Neural Computing Surveys*, 2:94–128.

Muller, R. (1996). A quarter century of place cells. *Neuron*, 17:813–822.

O'Reilly, R. C. and McClelland, J. L. (1994). Hippocampal conjunctive encoding, storage, and recall: avoiding a trade-off. *Hippocampus*, 4(6):661–682.

Wiskott, L. and Sejnowski, T. (2002). Slow feature analysis: Unsupervised learning of invariances. *Neural Computation*, 14(4):715–770.

Wyss, R., Konig, P., and Verschure, P. (2006). A model of the ventral visual system based on temporal stability and local memory. *PLOS Biology*, 4(5):e120.

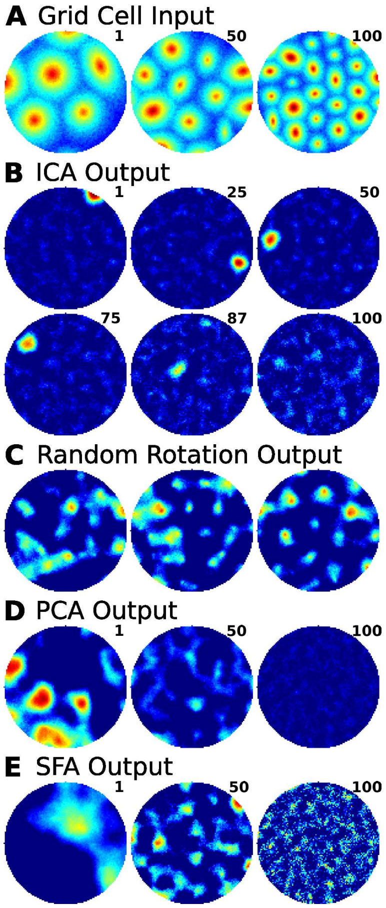

Figure 1: A: Spatial firing pattern (SFP) of the input units representing grid-cells. Three out of 100 units are shown. B: SFP of six out of 100 output units, computed by independent component analysis as a means of sparsification. Units are ordered by decreasing sparseness (kurtosis). Place fields of sparser units tend to have higher peak activity and are more often located at the border of the enclosure, whereas less sparse units tend to have multiple place fields. C: SFP of three out of 100 typical output units computed by random mixtures of the inputs. D: SFP of 1st, 50th, and 100th output computed by principal component analysis. E: SFP of 1st, 50th and 100th output computed by Slow Feature Analysis. Activities are color coded: red-high, green-medium, blue-zero activity. The full set of results can be viewed at http://itb.biologie.hu-berlin.de/~franzius/gridsToPlaces/